THE JOURNAL OF BIOLOGICAL CHEMISTRY VOL. 284, NO. 13, pp. 8777–8785, March 27, 2009
© 2009 by The American Society for Biochemistry and Molecular Biology, Inc. Printed in the U.S.A.

Timeless Maintains Genomic Stability and Suppresses Sister Chromatid Exchange during Unperturbed DNA Replication*[S]

Received for publication, August 7, 2008, and in revised form, December 8, 2008 Published, JBC Papers in Press, December 28, 2008, DOI 10.1074/jbc.M806103200

Karen A. Urtishak[‡], Kevin D. Smith[‡], Rebecca A. Chanoux[‡], Roger A. Greenberg[‡§], F. Brad Johnson[§], and Eric J. Brown[‡1]

From the [‡]Abramson Family Cancer Research Institute, Department of Cancer Biology, and the [§]Department of Pathology and Laboratory Medicine, University of Pennsylvania School of Medicine, Philadelphia, Pennsylvania 19104

Genome integrity is maintained during DNA replication by coordination of various replisome-regulated processes. Although it is known that Timeless (Tim) is a replisome component that participates in replication checkpoint responses to genotoxic stress, its importance for genome maintenance during normal DNA synthesis has not been reported. Here we demonstrate that Tim reduction leads to genomic instability during unperturbed DNA replication, culminating in increased chromatid breaks and translocations (triradials, quadriradials, and fusions). Tim deficiency led to increased H2AX phosphorylation and Rad51 and Rad52 foci formation selectively during DNA synthesis and caused a 3–4-fold increase in sister chromatid exchange. The sister chromatid exchange events stimulated by Tim reduction were largely mediated via a Brca2/Rad51-dependent mechanism and were additively increased by deletion of the Blm helicase. Therefore, Tim deficiency leads to an increased reliance on homologous recombination for proper continuation of DNA synthesis. Together, these results indicate a pivotal role for Tim in maintaining genome stability throughout normal DNA replication.

DNA synthesis utilizes complex sets of genes and functionalities to prevent genome maintenance failures. These potential failures include the misincorporation of nucleotides, the collapse of replication forks, and the formation of secondary structures that lead to chromosome deletions, duplications, and other mutagenic events (1–4).

In addition to polymerases and their cofactors, several higher order protein complexes act in concert during DNA replication to promote chromatin decondensation, DNA duplex unwinding, and protection of the resulting single-stranded DNA (ssDNA).[2] Failure to efficiently coordinate these processes can lead to stalling and collapse of the replication fork into double strand breaks (DSBs). For example, in budding yeast, deficiencies in DNA priming caused by low levels of pol α lead to a 22-fold increase in mitotic recombination (5). Similarly, in vertebrate cells, treatment with DNA polymerase inhibitors (*e.g.* aphidicolin) causes the generation of short segments of ssDNA, via polymerase-helicase uncoupling (6–11), and increases chromatid breaks at common fragile sites (12). The importance of polymerase processivity in genome stabilization raises the question to what degree the other components of the replication apparatus participate in genome maintenance.

Tim and its putative orthologs in yeast (Swi1 in *Schizosaccharomyces pombe* and Tof1 in *Saccharomyces cerevisiae*) facilitate DNA replication. Although less is known about Tim function in mammals, several functions of Swi1 and Tof1 have recently been described. Swi1 and Tof1 associate with chromatin and travel with the replication fork during S phase and are required for normal pausing at replication fork barriers (13–20). In addition, Tof1 associates with Cdc45 and MCM6, and deletion of Tof1 can lead to slowed replication fork progression (13, 17, 21).

Importantly, recent studies indicate that Swi1 and Tof1 coordinate DNA synthesis with DNA unwinding when replication is stalled (13). Using ChIP analysis, Tof1 deletion has been shown to cause the spatial uncoupling of replisome components from newly synthesized DNA when replication forks are stalled by hydroxyurea (HU) treatment. In addition, extended stretches of ssDNA have been observed in *swi1* mutants, consistent with uncoupling of DNA unwinding from synthesis (22). Finally, loss of Swi1 increases inter-sister recombination during S phase, as determined by the accumulation of X-shaped DNA structures in *swi1mus81* double mutants (15). These data, taken together, point to a role for Swi1 and Tof1 in both replisome maintenance and replication fork stability.

Several functions of Swi1 and Tof1 have been shown to be conserved either in Tim or in its vertebrate binding partner, Tipin. Tim and Tipin associate with chromatin as an interdependent complex (23) during S phase, putatively though the RPA34 binding domain of Tipin (24, 25). In addition, the Tim-Tipin complex associates with other components of the DNA replication apparatus, including Claspin, MCM subunits, pol δ, and pol ϵ (24, 26, 27). Furthermore, reduced expression of Tim

* This work was supported by the W. W. Smith Charitable Trust, American Cancer Society Institutional Grant IRG 78-002-29, and the Abramson Family Cancer Research Institute. The costs of publication of this article were defrayed in part by the payment of page charges. This article must therefore be hereby marked "*advertisement*" in accordance with 18 U.S.C. Section 1734 solely to indicate this fact.

[S] The on-line version of this article (available at http://www.jbc.org) contains supplemental Figs. 1 and 2.

[1] To whom correspondence should be addressed: 421 Curie Blvd., 514 BRB II/III, Philadelphia, PA 19104-6160. Tel.: 215-746-2805; Fax: 215-573-2486; E-mail: brownej@mail.med.upenn.edu.

[2] The abbreviations used are: ssDNA, single-stranded DNA; Tim, Timeless; SCE, sister chromatid exchange; DSB, double strand break; HU, hydroxyurea; shRNA, short hairpin RNA; HR, homologous recombination; MEF, murine embryonic fibroblast; FBS, fetal bovine serum; DMEM, Dulbecco's modified Eagle's medium; PBS, phosphate-buffered saline; PCNA, proliferating cell nuclear antigen; BrdUrd, bromodeoxyuridine; 7-AAD, 7-aminoactinomycin D.

slows DNA replication rates, as measured by cell cycle profile changes and DNA fiber labeling (24, 25, 27, 28). Consistent with a role for the Tim-Tipin complex in suppressing the accumulation of ssDNA at replication forks, pharmacological inhibition of DNA replication in Tipin-depleted *Xenopus* extracts leads to a 2-fold increase in chromatin-associated RPA (26).

Most studies to date have focused on the functions of Tim-Tipin under genotoxic stress (24–29). Although it is known that Tim can associate with the replisome components during S phase, and that its depletion leads to decreased rates of DNA synthesis, the role of Tim in genome stability during normal DNA replication is not well characterized. Here we demonstrate that Tim is required to maintain genome stability even in the absence of exogenous DNA-damaging agents. We show that Tim reduction leads to increased chromatid breaks, translocations, and inter-sister recombination events, as revealed by Rad52 and Rad51 focal accumulation and increased rates of sister chromatid exchange (SCE). Increased SCEs in Tim-deficient cells are at least partially dependent on Brca2 and Rad51, indicating that Tim dysfunction leads to an increased reliance on homologous recombination for continuation of DNA synthesis. These data demonstrate that Tim, an important component of the DNA replication apparatus, is required for maintaining genome integrity during unperturbed DNA replication.

EXPERIMENTAL PROCEDURES

Cell Culture—$Blm^{-/-}$ and $Rad52^{-/-}$ embryos were generated by intercrossing mice heterozygous for the $Blm^{tm1Grdn}$ and Rad52 null alleles, respectively (30, 31). $Blm^{-/-}$ and $Rad52^{-/-}$ murine embryonic fibroblasts (MEFs) were generated from E12.0 and E14.5 embryos, respectively, and immortalized by stable expression of SV40 large T antigen (32). MEFs and NIH3T3 cells were grown in Dulbecco's modified Eagle's medium (DMEM) containing 10% fetal bovine serum (FBS) in a 3% O_2 (5% CO_2) incubator. Stably expressing GFP-Rad52 cell lines were made by transducing NIH3T3 cells with LX-GFP-Rad52-N retrovirus (33).

Lentiviral ShRNA Infection—Short hairpin RNA (shRNA)-expressing lentiviral vectors targeting Tim (Tim #1, TRCN0000097985; Tim #5, TRCN0000097989), Brca2 (Brca2 #1, TRCN0000071011; Brca2 #2 TRCN0000071009), and Rad51 (Rad51 #1, TRCN0000012660; Rad51 #2, TRCN0000012661) were purchased from Open Biosystems. Control shRNA (5′-CCTAAGGTTAAGTCGCCCTCGCTCTAGCGAGGGCGACTTAACCTTAGG-3′) was derived from Addgene plasmid 1864 (34). For most experiments, the cassette encoding the puro resistance gene in these lentivirus vectors was replaced with enhanced green fluorescent protein to serve as a marker of infection rates. Lentiviral shRNAs were generated using a previously described packaging system (35). Cells were infected at a multiplicity of infection of 5–20 and collected 48–96 h after infection; transduction efficiencies were typically >95% as determined by enhanced green fluorescent protein detection. For NIH3T3 synchronization, cells were infected in 0.1% FBS/DMEM for 48 h, then stimulated with 10% FBS/DMEM, and collected at specified time points. Immortalized $Blm^{-/-}$, $Rad52^{-/-}$, and control MEFs were infected with shRNA-encoding lentiviruses in 0.1% FBS/DMEM. Twenty eight hours after infection, MEFs were stimulated with 10% FBS to re-enter the cell cycle.

BrdUrd Flow Cytometric Analysis—The percentage of cells in S phase (Fig. 1*B*) was quantified by pulsing similarly cultured NIH3T3 cells with 10 μM BrdUrd (Sigma) for 30 min. Cells were then fixed in 70% ethanol, and DNA was denatured using 3 N HCl, 0.5% Tween 20. Cells were stained with anti-BrdUrd antibodies (1:200, Pharmingen) for 20 min, followed by detection with fluorescein isothiocyanate-conjugated goat anti-mouse secondary antibodies (1:200, Pharmingen) and propidium iodide (2.5 μg/ml) for DNA content. BrdUrd-positive cells were quantified by flow cytometry using a FACSCalibur (BD Biosciences).

Western Blots and Quantitative Real Time PCR—Whole cell extracts were prepared by washing suspended cells with ice-cold PBS, followed by direct lysis in Laemmli sample buffer, and boiling for 5 min to denature proteins and DNA. Proteins were separated by SDS-PAGE and transferred to polyvinylidene difluoride (Millipore). Primary antibodies for protein detection include the following: anti-actin (1:2000, Santa Cruz Biotechnology, Inc.), anti-glyceraldehyde-3-phosphate dehydrogenase (1:2000, USBiological), anti-phospho-H2AX clone JBW301 (1:2000, Upstate), anti-Rad51 (1:500, Santa Cruz Biotechnology, Inc.), and anti-Stat3 (1:1000, Cell Signaling). The Timeless antibody (36) was generously provided by P. Minoo (University of Southern California, Los Angeles). Secondary horseradish peroxidase-conjugated species-specific antibodies were diluted 1:2000 (Santa Cruz Biotechnology, Inc.). For real time PCR quantification, RNA from $Rad52^{+/+}$ and $Rad52^{-/-}$ immortalized MEFs was isolated by TRIzol (Invitrogen) and chloroform extractions, and purified using an RNeasy kit (Qiagen). cDNA was prepared using a high capacity cDNA reverse transcription kit (Applied Biosystems). Primer and probes sets for β-actin (Mm 00607939 s1), Brca2 (Mm 00464783 m1), and Tim (Mm 00495610 m1) along with Taqman universal master mix were purchased from Applied Biosystems. Samples were run on an Applied Biosystems 7900HT Fast Real-Time PCR System, and data were analyzed using Applied Biosystems software.

Mitotic Spreads and SCE—For quantification of chromosome breaks, mitotic spreads were prepared as described previously (37) and stained with Giemsa. To visualize SCE, synchronized cells stimulated with 10% FBS were incubated with 10 μM BrdUrd (Sigma) for two consecutive S phases and treated with 0.5 μM nocodazole 3–4 h before collection. For aphidicolin treatment experiments, 0.2 μM aphidicolin (Calbiochem) was added prior to the second S phase in BrdUrd-containing media (15–16 h before nocodazole addition); 5 μM aphidicolin was added for 1 h, at a time point corresponding to the second S phase in BrdUrd-containing media, and was subsequently removed to allow cells to reinitiate cell cycle progression for 3 h before addition of nocodazole. For UV treatment experiments, cells in the second S phase of BrdUrd incorporation were treated with 5 or 10 J/m^2 UV light ($\lambda = 365$ nm) 4 h before the addition of nocodazole. Nocodazole-treated cells were resuspended by trypsinization, washed with PBS, incubated in 75 mM KCl for 20 min, fixed in methanol/acetic acid (3:1), and dropped onto prewarmed slides at 37 °C. Slides were incubated in 10 μg/ml Hoechst 33258 (Invitrogen) in H_2O for 20 min and then

washed in MacIlvaine solution (164 mM Na_2HPO_4, 16 mM citric acid, pH 7.0). Slides were then covered with glass coverslips and exposed to UV light ($\lambda = 365$ nm) for 30 min followed by a 1-h incubation in 1× SSC (20× = 3 M NaCl, 0.3 M Na_3citrate·$2H_2O$, pH 7.0) at 55 °C. Metaphase spreads were stained with Giemsa and visualized using an Olympus BX41 microscope (model U-DO3) with a 100× oil objective. SCEs and chromatid breaks were quantified from photographs taken with a Spot 3-shot insight QE camera (model 4.3) using Spot advanced software.

Cell Proliferation and Apoptosis Assays—Cells were infected in 10% FBS/DMEM. Twenty four hours later, cells were plated at low density in 6-well plates in triplicate for cell proliferation or on 6-cm dishes for apoptosis. Forty eight hours after plating, cell number was quantified using a Coulter Z2 counter or detected for apoptosis by staining with allophycocyanin-conjugated annexin-V (Pharmingen) and 7-AAD (Pharmingen) in 1× annexin-V binding buffer (10× = 0.1 M Hepes·NaOH, pH 7.4, 1.4 M NaCl, 25 mM $CaCl_2$) for 30 min. Apoptosis rates were determined by flow cytometry on a BD Biosciences FACSCalibur and gating for annexin-V positive/7-AAD negative events.

Immunofluorescence Staining—Cells were fixed at peak S phase, in 3% paraformaldehyde, 2% sucrose buffered with PBS or, for PCNA detection, in ice-cold methanol for 5 min, followed by 1 min in acetone. Cells were permeabilized in 0.5% Triton X-100/PBS for 20–60 min and immunostained with antibodies detecting PCNA (1:500, Santa Cruz Biotechnology, Inc.), γ-H2AX (1:1000, Upstate), and/or Rad51 (1:100, Santa Cruz Biotechnology, Inc.). Fluorophor-conjugated, species-specific secondary antibodies include the following: α-mouse Rhodamine Red and α-rabbit fluorescein isothiocyanate (Jackson ImmunoResearch) and α-rabbit Alexa Fluor 594 (Invitrogen), each diluted 1:1000. Foci were visualized by using a Nikon Eclipse E-800 microscope with a 100× oil objective. Rad51 and Rad52 foci, identified by significant distinction from nuclear background fluorescence, were quantified from images acquired using Metamorph software in Adobe Photoshop. Double blind methods were used for all quantifications.

Statistical Tests and Foci Quantification—For all figures, error bars represent standard errors, and *p* values were calculated by Student's *t* test. At least three independent replicates were performed for each experiment.

RESULTS

Tim Deficiency Increases Genomic Instability—Although Tim and Tipin have been shown to play partial roles in checkpoint responses to UV and HU treatment (24, 25, 27–29), they are also required for efficient DNA replication in the absence of such genotoxic stresses (24, 25, 27, 28). To investigate the role of Tim in maintaining genome stability during normal cellular proliferation, two independent shRNAs were used to reduce Tim expression to near undetectable levels in synchronized NIH3T3 cells (Fig. 1*A*). Genome stability was then assessed by two methods: H2AX phosphorylation and chromosome spreads. H2AX phosphorylation, a marker of DSB formation (38), was quantified in G_1-enriched cells (Fig. 1*B*, *1st* and *2nd lanes*) and in cells at peak S phase following growth factor stimulation (Fig. 1*B*, *3rd* and *4th lanes*). As expected, H2AX phosphorylation increased upon passage from G_1 into S phase in control cells (39); however, this increase was substantially enhanced by Tim reduction (Fig. 1*B*), consistent with the reported effect of Tipin knockdown (27). The increase in H2AX phosphorylation following Tim reduction was slightly greater than that observed following 1 gray ionizing radiation of asynchronous cells (data not shown), indicating that the level of DSB formation upon entry of Tim-deficient cells into S phase was considerable.

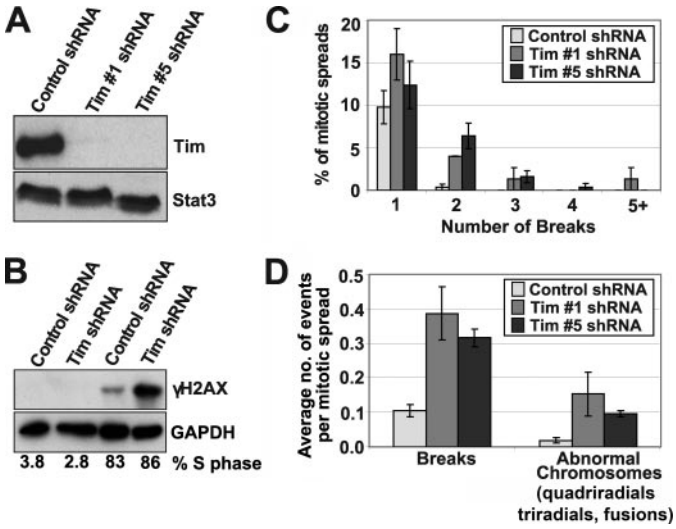

FIGURE 1. **Loss of Tim increases genomic instability.** *A*, Western blot quantification of Tim reduction in synchronized NIH3T3 cells using two independent shRNAs. Serum-starved cells were infected with control, Tim #1 or Tim #5 shRNA-expressing lentiviruses. 48 h after infection, cells were stimulated with growth factors to reenter the cell cycle, and Western blot samples were collected 2 days later. Total protein levels were normalized by BCA analysis prior to loading, and immunoblots were detected with anti-Tim antibodies. Stat3 was immunodetected as an additional loading and transfer control. *B*, Western blot analysis of phospho-H2AX levels in Tim knockdown cells during G_1 and S phase. Serum-starved NIH3T3 cells were infected with control or Tim #5 shRNA-expressing lentivirus as described in *A*, and protein samples were collected 6 h (G_1 cells) or 16–17 h (S phase) after growth factor stimulation. Phospho-H2AX was detected by immunoblot of total protein normalized samples, and anti-glyceraldehyde-3-phosphate dehydrogenase (*GAPDH*) was used as an additional loading control. The percentage of cells in S phase was determined by immunodetection of incorporated BrdUrd (30-min pulse), co-staining with propidium iodide, and gated quantification by flow cytometry. *C*, analysis of mitotic chromosome breaks following Tim reduction. Synchronized NIH3T3 were infected with lentiviruses expressing control, Tim #1 or Tim #5 shRNAs as described in *A*, and mitotic spreads were collected within 24 h after growth factor stimulation. Chromatid breaks were counted in 150 metaphases for each condition. *D*, quantification of chromatid breaks and abnormal chromosomes (triradials, quadriradials, and fusions) per metaphase upon Tim reduction. Differences between control and Tim-reduced cells were statistically significant (chromatid breaks, $p < 0.002$; abnormal chromosomes, $p < 0.02$).

To determine whether the instability caused by Tim reduction persisted into mitosis, chromosome spreads were prepared. Reduction of Tim expression utilizing two independent shRNAs resulted in a significant increase in chromatid breaks in comparison with controls (Fig. 1*C*, *D*). In addition, whereas control cells exhibited few abnormal chromosome structures (triradials, quadriradials, and fusions), Tim reduction caused a 5–7-fold increase in these types of chromosome rearrangements (Fig. 1*D*). Taken together, these data indicate that Tim reduction is sufficient to cause genomic instability in the absence of exogenous genotoxic stress.

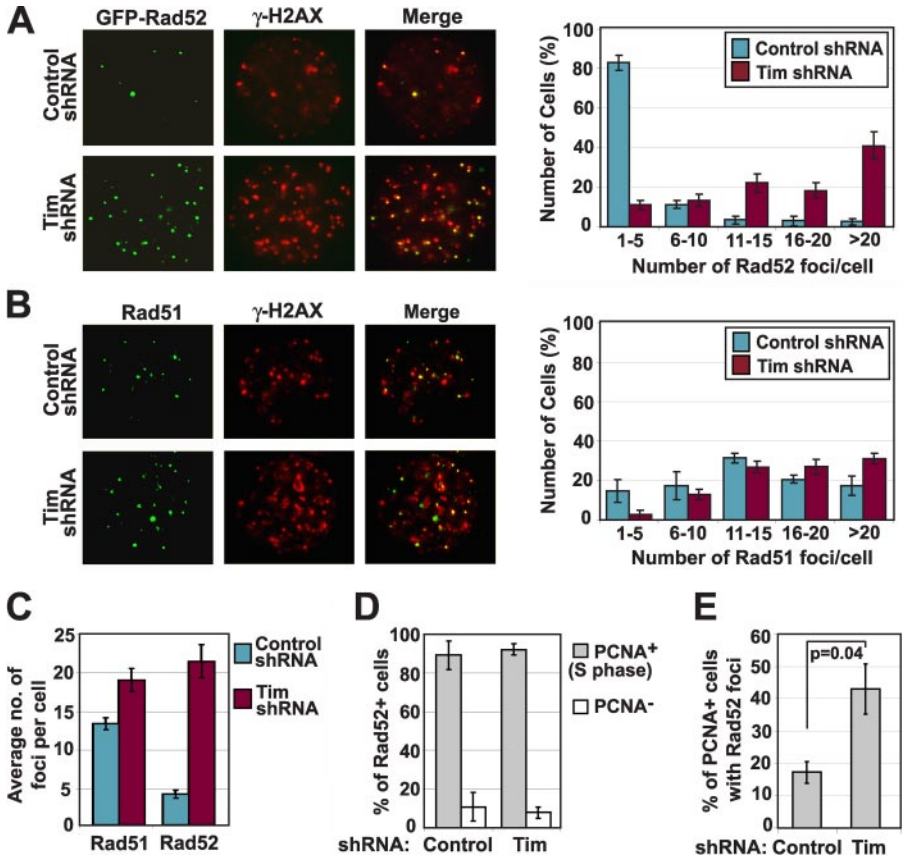

FIGURE 2. **Rad51 and Rad52 foci accumulate following Tim reduction.** *A*, analysis of Rad52 and γH2AX foci accumulation in NIH3T3 cells stably expressing GFP-Rad52. Serum-starved cells were infected with control or Tim #5 shRNA-expressing lentivirus as described in Fig. 1 and collected during peak S phase (16–17 h after growth factor stimulation). The number of Rad52 foci per cell was detected and quantified by GFP fluorescence; γH2AX was immunodetected using anti-phospho-H2AX antibodies. *B*, quantification of Rad51 foci in NIH3T3 cells expressing control or Tim #5 shRNAs. Cells were collected as in *A* and immunodetected for Rad51 and γH2AX, and the number of Rad51 foci per cell was determined. *C*, quantification of the average number of Rad51 and Rad52 foci from *A* and *B*. A statistically significant increase in Rad51 ($p = 0.007$) and Rad52 ($p < 0.00001$) foci was observed in Tim-reduced cells compared with controls. *D*, quantification of S phase and non-S phase cells exhibiting Rad52 foci. Tim-reduced and control cells, generated as described in *A*, were immunodetected for PCNA. GFP-Rad52 and PCNA positive cells were quantified. Only cells with abundant PCNA staining were scored as S phase cells. *E*, quantification of the percentage of PCNA-positive cells exhibiting Rad52 foci.

Tim Reduction Increases Rad51 and Rad52 Foci Formation during S Phase—Previous studies have shown that abnormalities during DNA replication can lead to DSB formation through replication fork collapse, causing a reliance on homologous recombination (HR)-mediated restart mechanisms (40). In addition, Rad52-dependent HR has also been proposed to counter the untoward effects of ssDNA accumulation upon helicase-polymerase uncoupling (15).

To assess whether Tim reduction leads to the accumulation of factors that participate in HR, Rad51 and Rad52 foci formation were quantified (41–43) in synchronized NIH3T3 cells. As shown in Fig. 2*A*, Tim reduction led to a significant increase in cells exhibiting high numbers of Rad52 foci, as determined by visualization of stably expressed GFP-Rad52. In contrast to controls, which generally exhibited few foci (<5 per cell), the vast majority of Tim knockdown cells (89.1%) had greater than 5 Rad52 foci, with 41.0% exhibiting more than 20 foci per cell. Rad52 foci predominantly overlapped with γH2AX (86.8% in control cells and 92.4% in Tim knockdown cells), indicating that Rad52 foci formed at sites of DNA damage. On average, 4.3 and 21.5 Rad52 foci were observed in control and Tim-deficient cells, respectively, a 5.7-fold increase (Fig. 2*C*).

Rad51 foci also overwhelmingly overlapped with phospho-H2AX (>92%) and were increased in Tim knockdown cells, although more modestly in comparison with Rad52 foci (Fig. 2*B*). In comparison with controls, a significant increase ($p < 0.05$) in Rad51 foci was observed only in Tim knockdown cells with >20 Rad51 foci per cell. On average, 13.3 Rad51 foci were observed in control cells compared with 19.0 foci in Tim knockdown cells (Fig. 2*C*), a 1.5-fold increase. Thus, a lesser absolute number of Rad51 foci was stimulated by Tim reduction in comparison with Rad52 foci (5.7 Rad51 *versus* 17.2 Rad52). This result combined with the frequency of Rad51 and Rad52 overlap (controls, 58.7% ± 4.8, and Tim-deficient, 53.2% ± 3.2; supplemental Fig. 1) suggest that only approximately half the Rad52 foci that formed as a consequence of Tim reduction were accompanied by Rad51.

To determine whether foci formation occurred during DNA synthesis, GFP-Rad52-expressing cells were stained for PCNA. Indeed, nearly all cells, either control or Tim knockdown, that exhibited Rad52 foci also had profuse PCNA staining, a hallmark of S phase (89.1% for control and 92.2% with Tim reduction; Fig. 2*D*). As expected, the percentage of S phase cells with Rad52 foci increased significantly in Tim-reduced cells compared with controls (Fig. 2*E*). Taken together, these results indicate that Tim reduction increases Rad51 and Rad52 foci, and that Rad52 foci form during S phase.

Sister Chromatid Exchange Increases with Tim Reduction—The increase in Rad52 and Rad51 foci in Tim-reduced cells (Fig. 2, *A* and *B*) raised the question whether the chromosomal abnormalities observed (Fig. 1, *C* and *D*) under-represented the frequency of genomic instability resulting from Tim deficiency and that HR effectively counters such instability in S phase. SCE detects recombinatorial repair events between sister chromatids during the S and G_2 phases of the cell cycle and are generated by the resolution of HR intermediates (Holliday junctions) in a manner that causes crossovers (2). Recombination structures that lead to SCEs can arise during replication fork restart following collapse (2) and, purportedly, as a means to compensate for extended lagging strand gaps (15).

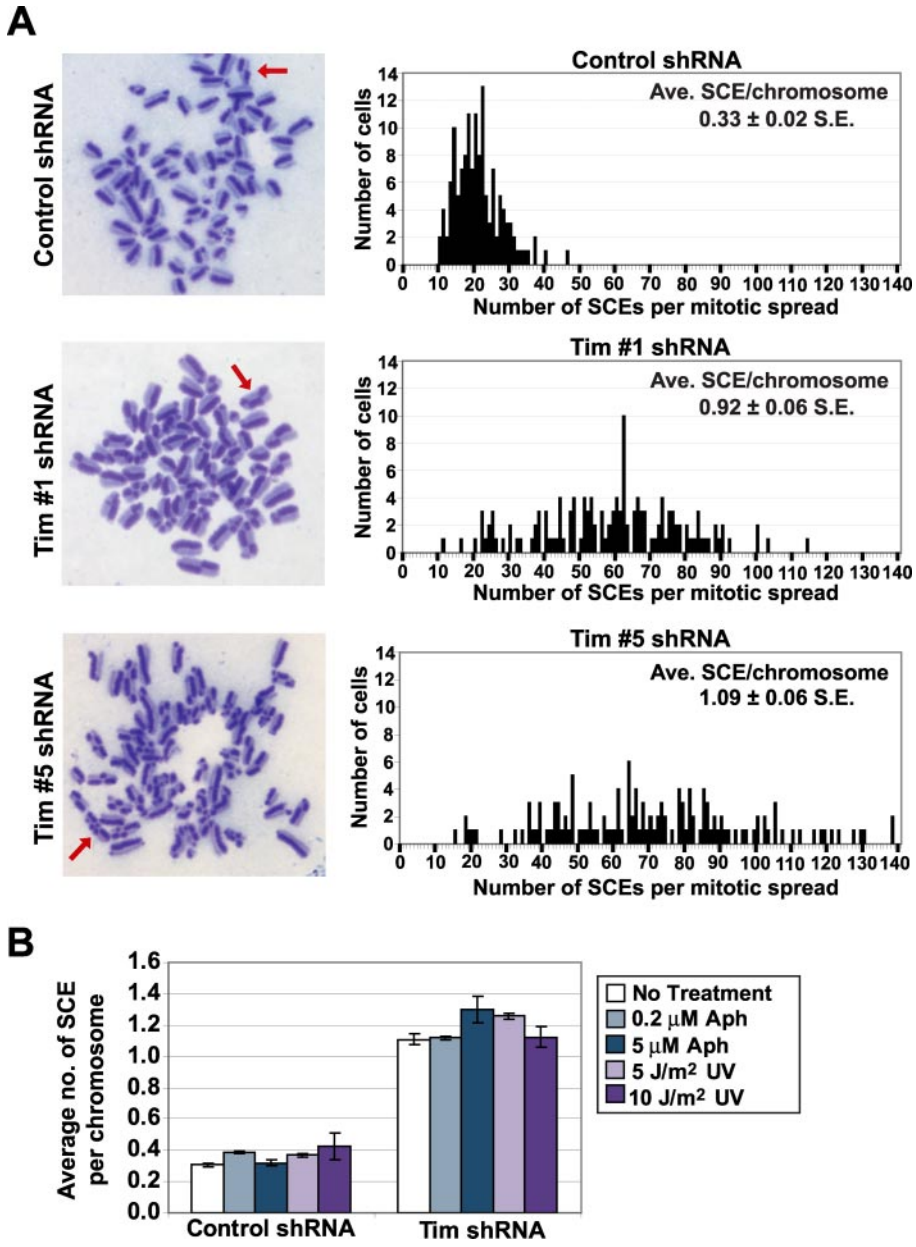

FIGURE 3. **Tim suppresses sister chromatid exchange.** *A,* spontaneous SCE levels in synchronized NIH3T3 cells infected with control, Tim #1, or Tim #5 shRNA-expressing lentiviruses. Cells were incubated with BrdUrd for two rounds of replication and collected for mitotic spreads. SCEs were counted in at least 135 metaphases for each condition. Representative metaphases for each lentivirus are shown; *arrows* indicate examples of chromosomes with SCEs. The number of SCEs per mitotic spread is graphically represented (*left panels*); the average SCEs per chromosome and standard errors are shown. The observed increase in SCEs per chromosome upon Tim reduction in comparison with controls was statistically significant ($p < 0.0001$). *B,* quantification of SCE in NIH3T3 cells expressing control or Tim #5 shRNAs following replication stalling or DNA damage. A statistically significant increase in SCE levels was observed in control cells treated with 0.2 μM aphidicolin or 5 J/m^2 UV ($p < 0.02$). SCE rates in Tim-reduced cells were dramatically higher than all treated and untreated controls ($p < 0.0001$). SCE levels in Tim-deficient cells treated with 5 μM aphidicolin and 5 J/m^2 UV were significantly different from untreated Tim-deficient cells ($p < 0.05$); however, SCEs levels observed following all other treatments of Tim-deficient cells were not significantly different from untreated Tim-deficient cells.

SCE frequency was determined in synchronized NIH3T3 control and Tim-reduced cells as a means to assess HR-mediated repair. As shown in Fig. 3*A*, the number of SCEs per mitotic spread increased more than 3-fold upon Tim reduction. Tim #1 and Tim #5 shRNAs increased the number of SCEs per chromosome from 0.33 in wild-type controls to 0.92 and 1.09 in Tim knockdown cells, respectively. Thus, Tim is required to prevent recombination events that lead to SCEs.

Tim deficiency has previously been shown to slow DNA replication (24, 25, 27, 28). We next sought to compare the rate of SCE caused by Tim deficiency with that caused by other treatments known to inhibit replication rates, specifically aphidicolin and UV light exposure (Fig. 3*B*). Consistent with previous findings, low dose aphidicolin and UV treatment caused marginal, but statistically significant, increases in SCE rates in wild-type cells ($p = 0.0007$ and 0.015, respectively). However, these increased rates of SCE were far less than that caused by Tim reduction alone (Fig. 3*B*). Moreover, treatment of Tim-deficient cells with low dose aphidicolin (0.2 μM), pulsed high-dose aphidicolin, or UV light exposure did not appreciably increase SCEs, indicating that the inherent role of Tim in preventing recombination events in S phase is not associated with excessive DNA damage or polymerase stalling. Together, these studies strongly argue that Tim has an important function in preventing recombination events during unperturbed DNA replication.

Tim and Blm Are Non-epistatic—Bloom syndrome, caused by a mutation in the *BLM* gene, is characterized by increased frequencies of chromosomal aberrations (chromatid breaks, triradials, and quadriradials) and, in particular, SCEs (44, 45). As a member of the RecQ helicase family, Blm aids in Holliday branch migration and a resolution pathway that does not lead to SCE (46–48). The cytogenetic similarities between Blm mutants and Tim-reduced cells, in conjunction with recent studies implying regulation of Blm through the ATR-Chk1 pathway (49, 50), led us to investigate whether increased SCEs in Tim-deficient cells was partly attributable to Tim and Blm functioning in the same pathway.

To examine Tim and Blm epistasis, Tim protein levels were reduced by shRNA (Fig. 4*A*) in transformed Blm wild-type and null MEFs. Changes in proliferation rates in Blm$^{+/+}$ and Blm$^{-/-}$ MEFs 72 h (~3 doublings) after lentiviral infection were determined. Although Tim reduction in Blm$^{+/+}$ MEFs led to a 2.1-fold reduction in proliferation in comparison with control shRNA-expressing Blm$^{+/+}$ and Blm$^{-/-}$ MEFs, Tim sup-

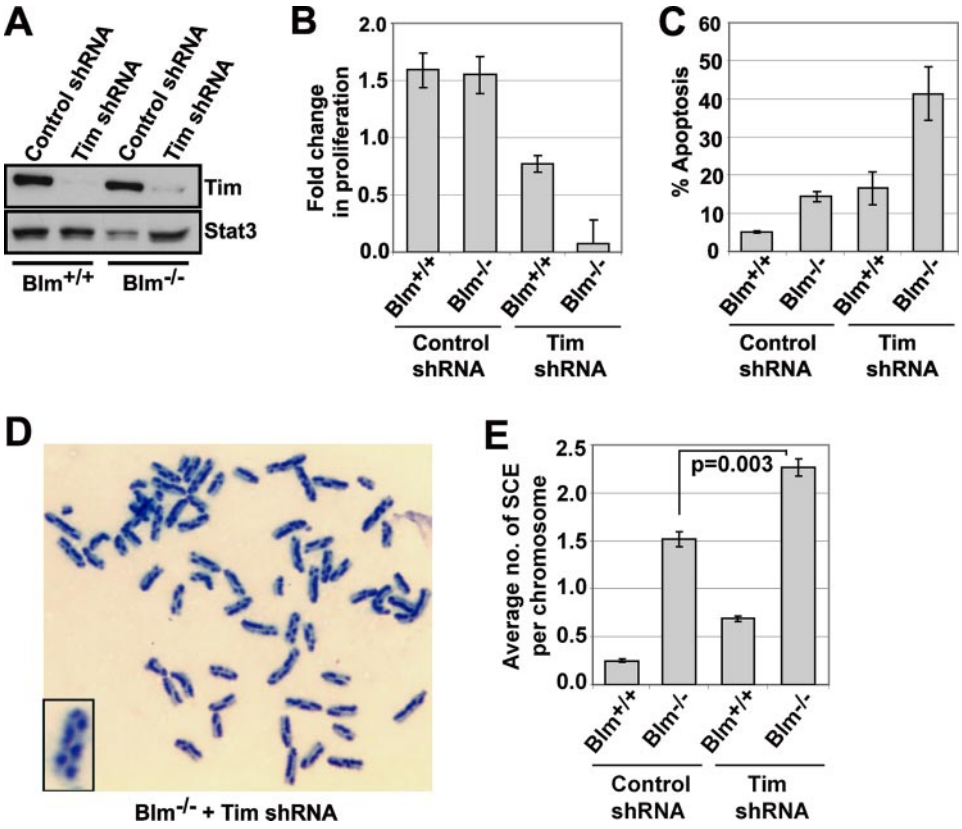

FIGURE 4. **Tim and Blm perform distinct functions.** *A*, Western blot quantification of Tim knockdown efficiency in transformed Blm$^{+/+}$ and Blm$^{-/-}$ MEFs. Protein samples were collected 48 h after infection. Immunodetection was performed using anti-Tim and anti-Stat3 antibodies. *B*, quantification of cell proliferation. Cells were infected with control or Tim #5 shRNA-expressing lentiviruses. Twenty four hours after infection, cells were replated at low density and counted 48 h later. A statistically significant decrease in proliferation was found between Blm$^{+/+}$ and Blm$^{-/-}$ MEFs infected with Tim #5 shRNA-expressing lentiviruses ($p = 0.03$). *C*, analysis of apoptosis rates. Cells were infected with control or Tim #5 shRNA-expressing lentiviruses and co-stained with allophycocyanin-annexin-V and 7-AAD 72 h after infection; annexin-V-positive and 7-AAD-negative cells were scored as apoptotic. A statistically significant increase in apoptosis was found comparing Blm$^{+/+}$ and Blm$^{-/-}$ MEFs infected with Tim #5 shRNA-expressing lentivirus ($p = 0.02$). *D*, example of SCE rates in Blm$^{-/-}$ MEFs expressing Tim #5 shRNA. The *enlarged inset* shows a chromosome with five SCEs, a level of SCE that was frequently observed in Tim-reduced Blm$^{-/-}$ MEFs. *E*, quantification of SCEs per chromosome in transformed Blm$^{+/+}$ and Blm$^{-/-}$ MEFs expressing control or Tim #5 shRNAs. A statistically significant increase in SCEs per chromosome for Blm$^{-/-}$ cells expressing Tim #5 shRNA was observed compared with similar cells expressing control shRNA ($p = 0.003$).

pression in Blm$^{-/-}$ MEFs reduced proliferation 19.4-fold (Fig. 4*B*). To determine whether increased cell death contributed to the proliferative failure of Tim-deficient Blm$^{-/-}$ MEFs, apoptotic cells were quantified 72 h after infection (~3 cell doublings). Although apoptosis was slightly elevated in cells deficient for Tim or Blm alone in comparison with wild-type controls (Fig. 4*C*), the frequency of apoptotic cells increased 8-fold in Tim-reduced Blm$^{-/-}$ MEFs over wild-type controls. These results indicate that combined deficiency in Tim and Blm causes synthetic lethality.

To investigate whether Tim and Blm suppress inter-sister recombination as part of the same or distinct pathways, SCE analysis was performed in Tim-deficient Blm wild-type and null MEFs. To avoid any potential confounding effects of proliferative failure and apoptosis, SCEs were analyzed at an earlier point after Tim reduction (~2 cell doublings). Indeed, reduction of Tim in Blm$^{-/-}$ cells increased SCE rates to levels greater than that observed under any other condition (Fig. 4, *D* and *E*). Tim reduction in Blm$^{-/-}$ MEFs led to a rate of SCE (2.26 SCEs per chromosome) that was significantly greater than that observed in either Tim-reduced Blm$^{+/+}$ cells or control shRNA-infected Blm$^{-/-}$ cells (Fig. 4*E*), which exhibited SCE levels similar to previous determinations (Fig. 3) (51, 52). Of note, it is likely that the SCE rate in Tim-deficient Blm$^{-/-}$ MEFs is an underestimate of the actual SCE level, as it was near the upper limit of quantification (Fig. 4*D*, *inset*) and may have been influenced by inhibition of metaphase formation in the most severely affected cells. These results indicate that Tim and Blm perform distinct functions in suppressing SCE rates. Thus, the function of Tim in preventing recombination in S phase likely lies in avoiding the formation of recombination intermediates and not in regulating Blm-mediated resolution.

Sister Chromatid Exchange in Tim-deficient Cells Is Dependent on Brca2 and Rad51—Previous studies in *S. pombe* suggest that recombination events generated in *swi1* mutants require Rad22 (mammalian Rad52 homolog), purportedly to anneal parent strands within extended lagging strand gaps in a Rad51-independent manner (15). Our results suggest that recombination events generated by Tim deficiency could be through a similar mechanism as in yeast because both Rad52 foci and SCE increased significantly when Tim was reduced.

To assess if inter-sister recombination in Tim-reduced cells requires Rad52, we determined SCE rates in transformed Rad52$^{+/+}$ and Rad52$^{-/-}$ MEFs. Once again, Tim reduction led to a 3–4-fold increase in SCE in Rad52$^{+/+}$ MEFs in comparison with control shRNA-infected Rad52$^{+/+}$ and Rad52$^{-/-}$ MEFs (Fig. 5*A*). However, the absence or presence of Rad52 led to no significant differences in either SCE rates (Fig. 5*A*) or the number of chromatid breaks generated upon Tim reduction (Fig. 5*B*). These results demonstrate that recombination events generated by loss of Tim are not dependent on Rad52, and suggest that Tim deficiency in mammals leads to recombination via mechanisms distinct from those operating in *swi1* mutants.

SCEs can also result from the HR-mediated reinitiation of replication forks that have collapsed into DSBs. These repair events are highly dependent on Rad51 (2). In addition, Brca2, a putative mammalian counterpart to yeast Rad52, facilitates recruitment of Rad51 to resected DSBs (53) and has also been shown to play a key role in replication fork recovery (54).

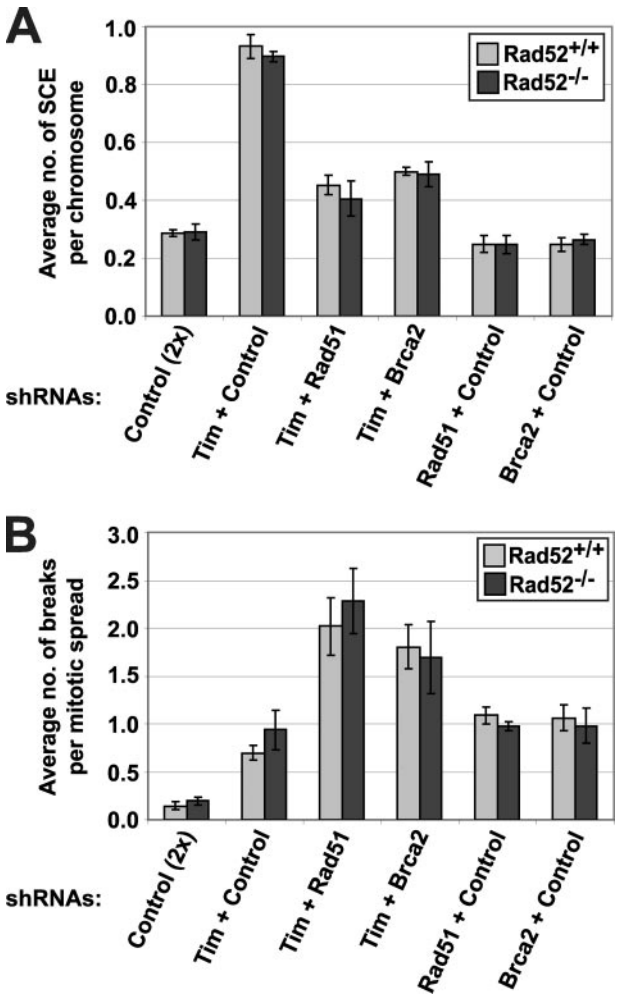

FIGURE 5. **SCE requires Brca2 and Rad51 in Tim-reduced cells.** *A*, quantification of average SCEs per chromosome in transformed Rad52$^{+/+}$ and Rad52$^{-/-}$ MEFs expressing control or Tim #5 shRNAs in combination with Brca2 #1 or Rad51 #1 shRNAs. At least 30 metaphases were scored for each condition. SCEs levels in Tim-reduced (*Tim #5 + Control shRNA*) Rad52$^{+/+}$ and Rad52$^{-/-}$ cells were significantly greater than all other conditions, including ones in which Rad51 or Brca2 expression was suppressed ($p < 0.001$). *B*, number of breaks per mitotic spread following reduction of Tim combined with reduction of Rad51 or Brca2. Breaks were quantified in both synchronized Rad52$^{+/+}$ and Rad52$^{-/-}$ MEFs. At least 40 metaphases were scored for each condition. A significant increase in the number of breaks was observed in Rad51 + Tim shRNA-expressing cells in comparison with cells expressing Rad51 or Tim shRNAs alone ($p \leq 0.025$). *p* values testing the significance of the increased the number of breaks for Rad52$^{+/+}$ and Rad52$^{-/-}$ cells expressing Brca2 + Tim shRNAs compared with Brca2 or Tim shRNAs alone were $p \leq 0.03$ (Rad52$^{+/+}$) and $p < 0.13$ (Rad52$^{-/-}$).

To determine whether Rad51 and Brca2 mediate SCEs stimulated by Tim deficiency, Rad51 and Brca2 levels were suppressed by shRNA expression in combination with Tim reduction (supplemental Fig. 2, *A* and *B*). Strikingly, the majority of the SCEs resulting from Tim deficiency were suppressed by reduction of Rad51 or Brca2 (Fig. 5*A*). Similar effects were observed utilizing independent shRNAs targeting different regions of the Rad51 and Brca2 transcripts (supplemental Fig. 2*C*). Complete suppression of SCE in Tim-deficient cells was not achieved by Rad51 or Brca2 reduction (Fig. 5*A*), even in the absence of Rad52 (Rad52$^{-/-}$, Fig. 5*A*). These results argue against Rad52 playing a minor compensatory function in SCE under conditions of Rad51 or Brca2 suppression. The inability of shRNA-mediated suppression of Rad51 and Brca2 to prevent all SCEs could be due to incomplete protein reduction (supplemental Fig. 2, *A* and *B*) or reflect the existence of an unknown alternative pathway that is required for this minor fraction of recombination events following Tim reduction.

Failure to undergo HR-mediated repair in Rad51-deficient cells, as indicated by reduced SCEs, would be predicted to lead to persistence of DSBs. Consistent with this expectation, dual suppression of Tim and Rad51 significantly increased chromatid breaks (Fig. 5*B*). Similar trends were observed upon Brca2 suppression (Fig. 5*B*). Together, these data strongly argue that Tim deficiency leads to a reliance on Rad51- and Brca2-mediated HR repair to maintain genome stability in S phase.

DISCUSSION

Prevention and repair of DNA damage during DNA replication is crucial for maintaining genome integrity and cell viability. Replisome deregulation can lead to genome instability, both through replication fork collapse and the generation of single strand gaps created by the uncoupling of polymerases from helicases (1, 6, 55). In this study, we find that Tim, a regulator of DNA replication efficiency (24, 25, 27, 28), suppresses DSBs and chromosome abnormalities during unperturbed DNA synthesis. Furthermore, we demonstrate that Tim deficiency results in an increased reliance on the HR repair factors, Rad51 and Brca2, to mediate SCE and maintain genome stability. Because the stimulatory effect of Tim reduction on SCE far exceeds that caused by exogenous DNA damage or replication inhibitors, the function of Tim in preventing recombination events during DNA synthesis is considerable, even during normal replication.

Previously, the Tim-Tipin complex has been shown to interact with proteins in the replisome and influence both Chk1 phosphorylation and the intra-S phase checkpoint in response to genotoxic stress (23–29). Because deficiencies in the ATR-Chk1 checkpoint pathway lead to increased DSB formation (3), the facilitative role of Tim in Chk1 regulation under genotoxic conditions raises the possibility that the checkpoint function of Tim is the sole mechanism by which Tim/Tipin suppresses recombination during normal S phase. However, several lines of evidence argue against this possibility. First, although a partial decrease in Chk1 phosphorylation (≥50%) has been reported in Tim- and/or Tipin-deficient cells under conditions of genotoxic stress, the basal levels of Chk1 phosphorylation in unchallenged cells either has been shown to increase or not change appreciably (25, 26, 28, 29). Increased Chk1 phosphorylation in Tim-deficient cells is in fact expected, given evidence both in yeast and *Xenopus* extracts that Tim/Tipin deficiency leads to the accumulation of ssDNA during DNA replication (15, 22, 26), which stimulates the ATR-Chk1 pathway (3). Therefore, the function of Tim in preventing DSBs during unperturbed S phase does not appear to be solely linked to assisting Chk1 activation under genotoxic stress.

Evidence both in yeast and vertebrates suggests that ssDNA accumulation resulting from defects in replisome efficiency may be the root cause of genome instability in Tim-reduced cells. For example, using ChIP analysis, it has been shown that

Tof1 is required to maintain coupling between helicase complexes (Cdc45 and MCM7) and newly synthesized daughter strands following HU treatment of *S. cerevisiae* (13). Deficiencies in coupling were correlated with an expansion of RPA-coated DNA, a hallmark of ssDNA generation. These effects were not observed in *mec1tel1sml1* mutants, arguing against checkpoint deficiency being the primary cause of uncoupling (13). Generation of ssDNA has also been observed in *swi1* and *swi3* mutants, *S. pombe* orthologs of Tim and Tipin (22), and in Tipin-depleted *Xenopus* extracts (26). Together these data argue that primary genome stabilizing function of Tim in S phase is to ensure that daughter strand synthesis remains coupled to helicase progression. Loss of this capability alone, or in combination with partial checkpoint reduction, likely contributes to DSB formation in Tim-depleted cells.

Because we observed that the rate of SCE seen in Tim-reduced Blm$^{-/-}$ cells was greater than that observed in cells deficient for either protein alone, our results indicate that Tim deficiency does not lead to increased SCEs through a defect in Blm function. Furthermore, dual deficiency in Tim and Blm results in a decrease in cell proliferation and an increase in apoptosis, consistent with the growth defects observed upon combined mutation of yeast orthologs of Tim (Swi1 and Tof1) with Blm counterparts (Rqh1 and Sgs1) (14, 56). Blm, a RecQ helicase, aids in Holliday junction migration and resolution, which in turn suppress sister chromatid crossover events (46–48). Our studies are consistent with the hypothesis that Tim reduction leads to an increased frequency of Holliday junctions, which can undergo Blm-mediated migration and coalescence to suppress SCE (Fig. 6). Previous studies have indicated that the formation of recombination structures in S phase is associated with decreased rates of DNA synthesis (57). Thus, it is possible that increased recombination contributes to the slowed rate of DNA synthesis previously noted in Tim-deficient cells (24, 25, 27, 28).

An important study of Tim and Tipin orthologs in *S. pombe* has indicated that increased recombination in Swi1 and Swi3 mutant strains occurs independently of DSB generation and Rad51 (15). This study demonstrated that combined deletion of Swi1 and Mus81 (a protein required for Holliday junction resolution) caused the accumulation of unresolved recombination intermediates in a manner that was dependent on Rad22 (mammalian Rad52). Rad22 mutation, but not mutation of Rhp51 or Rhp54 (mammalian Rad51 and Rad54), suppressed *swi1 mus81* synthetic lethality. From these data, the authors proposed that the absence of Swi1 during replication leads to replisome uncoupling from newly synthesized DNA, resulting in single strand gaps in the lagging strand that are predominantly repaired by exchange events between the intact parental strands (15). According to this model, fork collapse and DSB formation are averted by the single strand annealing function of Rad22, implying an important specific function in replication fork stability that does not involve Rad51 recruitment (Fig. 6).

Although Rad52 is required for HR in yeast, it is dispensable in mammals, and its loss has little effect on cell viability (31, 41, 42, 58). This difference is largely attributed to the existence of genes that function redundantly with Rad52 in recruiting Rad51 to breaks. These Rad52 analogs include Brca2 and Xrcc3

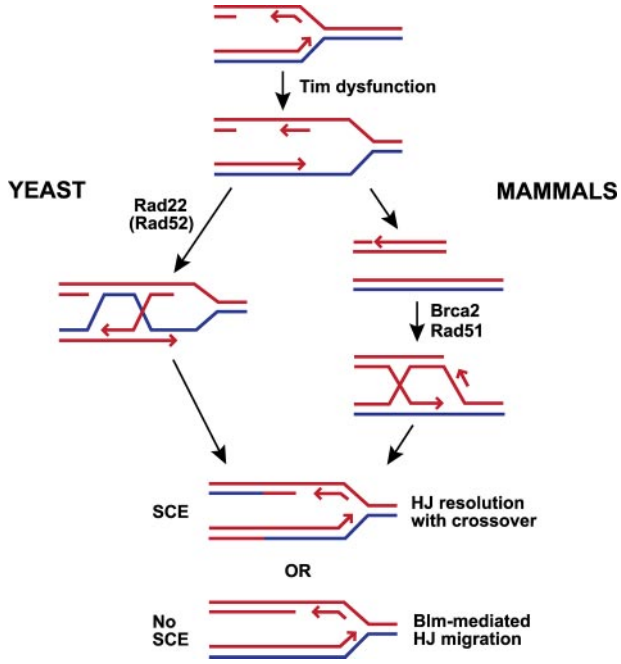

FIGURE 6. **A model depicting the generation of SCEs by Tim reduction.** Tim dysfunction during DNA replication leads altered replication fork configurations that lead to SCE. In *S. pombe*, altered forks resulting from mutation of Tim/Tipin orthologs cause further processing by a Rad22-dependent mechanism, generating Holliday junctions (15). In mammals, Tim dysfunction may lead to some fraction of replication forks to collapse into DSBs and be restarted subsequently through Brca2/Rad51-dependent mechanisms (*right side*). Through less defined processes, Rad51 and Brca2 may also function in preventing fork collapse by generating structures similar to those generated in *S. pombe*. In either species, Holliday junctions can be resolved in a manner that generates crossovers (SCE) or undergo Blm-mediated migration into adjacent junctions to suppress SCE. It is conceivable that Blm may also suppress SCE in Tim-deficient cells through migration of regressed forks before collapse (15), thus averting Holiday junction resolution into DSBs and the Rad51/Brca2-dependent restart pathway shown above.

(41, 43, 59). However, such redundancy in Rad51 recruitment would not exclude a specific role for Rad52 in mediating exchange through single strand annealing, which appears to be conserved in vertebrate cells (60, 61). However, Tim knockdown in Rad52$^{-/-}$ cells had no significant effect on SCE rates or the appearance of chromatid breaks. Thus, unlike in yeast, Tim reduction does not induce a dependence on Rad52 for recombinatorial exchange.

Our results indicate that in mammals Rad52 is not required for SCE or genome maintenance in Tim-deficient cells. Instead, Rad51-mediated SCE is utilized as means to avert the genomic instability resulting from Tim absence (Fig. 6). Interestingly, our data also indicate a prominent role for Brca2 in this process, consistent with the proposed role for Brca2 as a functional equivalent to yeast Rad52. A Rad51/Brca2-dependent process that averts fork collapse by mechanisms similar to *S. pombe* should not be excluded. However, given the increase in chromatid breaks and phosphorylation of H2AX in response to Tim deficiency (Figs. 1, 2, and 5), and the known functions of Brca2 and Rad51 in DNA repair, our data suggest that some fraction of SCEs observed in Tim-deficient cells are the product of replication fork collapse into DSBs (Fig. 6). Together, these results indicate that Tim deficiency leads to a reliance on Brca2- and Rad51-mediated repair for genome stability during normal DNA replication.

Although the mechanisms governing SCE are becoming increasingly understood, only a handful of genes that influence this process have been identified (2). One of these genes, Blm, leads to a >150-fold increase in cancer risk when mutated in humans. Importantly, the cytogenetic abnormalities (chromatid breaks, quadriradials, and triradials) and sister chromatid exchange rates observed in Blm null cells (30, 51, 52, 62) are only modestly greater than those observed in Tim-reduced cells (Fig. 3). Thus, it is conceivable that Tim, Tipin, and other yet to be described genes that contribute to replisome efficiency, may be important for suppressing cancer in humans. Furthermore, in light of our studies, it is conceivable that the penetrance of cancer-causing mutations in HR regulators, such as Blm and Brca2, may be strongly influenced by mutation of Tim or Tipin.

Acknowledgments—We are grateful to the following individuals for generously providing reagents: Parviz Minoo (anti-Tim antibody); Joanna Groden ($Blm^{tm1Grdn/+}$ mice); Albert Pastink and Maria Jasin ($Rad52^{-/-}$ null mice); Nancy Maizels (GFP-Rad52 expression construct); and David Sabatini (Addgene plasmid 1864).

REFERENCES

1. Tourriere, H., and Pasero, P. (2007) *DNA Repair* **6,** 900–913
2. Wilson, D. M., III, and Thompson, L. H. (2007) *Mutat. Res.* **616,** 11–23
3. Paulsen, R. D., and Cimprich, K. A. (2007) *DNA Repair* **6,** 953–966
4. Aguilera, A., and Gomez-Gonzalez, B. (2008) *Nat. Rev. Genet.* **9,** 204–217
5. Lemoine, F. J., Degtyareva, N. P., Lobachev, K., and Petes, T. D. (2005) *Cell* **120,** 587–598
6. Nedelcheva-Veleva, M. N., Krastev, D. B., and Stoynov, S. S. (2006) *Nucleic Acids Res.* **34,** 4138–4146
7. Michael, W. M., Ott, R., Fanning, E., and Newport, J. (2000) *Science* **289,** 2133–2137
8. Mimura, S., Masuda, T., Matsui, T., and Takisawa, H. (2000) *Genes Cells* **5,** 439–452
9. Walter, J. C. (2000) *J. Biol. Chem.* **275,** 39773–39778
10. Lupardus, P. J., Byun, T., Yee, M. C., Hekmat-Nejad, M., and Cimprich, K. A. (2002) *Genes Dev.* **16,** 2327–2332
11. Zou, L., and Elledge, S. J. (2003) *Science* **300,** 1542–1548
12. Durkin, S. G., and Glover, T. W. (2007) *Annu. Rev. Genet.* **41,** 169–192
13. Katou, Y., Kanoh, Y., Bando, M., Noguchi, H., Tanaka, H., Ashikari, T., Sugimoto, K., and Shirahige, K. (2003) *Nature* **424,** 1078–1083
14. Noguchi, E., Noguchi, C., Du, L. L., and Russell, P. (2003) *Mol. Cell. Biol.* **23,** 7861–7874
15. Noguchi, E., Noguchi, C., McDonald, W. H., Yates, J. R., III, and Russell, P. (2004) *Mol. Cell. Biol.* **24,** 8342–8355
16. Krings, G., and Bastia, D. (2004) *Proc. Natl. Acad. Sci. U. S. A.* **101,** 14085
17. Tourrière, H., Versini, G., Cordón-Preciado, V., Alabert, C., and Pasero, P. (2005) *Mol. Cell* **19,** 699–706
18. Calzada, A., Hodgson, B., Kanemaki, M., Bueno, A., and Labib, K. (2005) *Genes Dev.* **19,** 1905–1919
19. Mohanty, B. K., Bairwa, N. K., and Bastia, D. (2006) *Proc. Natl. Acad. Sci. U. S. A.* **103,** 897–902
20. Hodgson, B., Calzada, A., and Labib, K. (2007) *Mol. Biol. Cell* **18,** 3894–3902
21. Nedelcheva, M. N., Roguev, A., Dolapchiev, L. B., Shevchenko, A., Taskov, H. B., Shevchenko, A., Francis Stewart, A., and Stoynov, S. S. (2005) *J. Mol. Biol.* **347,** 509–521
22. Sommariva, E., Pellny, T. K., Karahan, N., Kumar, S., Huberman, J. A., and Dalgaard, J. Z. (2005) *Mol. Cell. Biol.* **25,** 2770–2784
23. Gotter, A. L. (2003) *J. Mol. Biol.* **331,** 167–176
24. Gotter, A. L., Suppa, C., and Emanuel, B. S. (2007) *J. Mol. Biol.* **366,** 36–52
25. Unsal-Kacmaz, K., Chastain, P. D., Qu, P. P., Minoo, P., Cordeiro-Stone, M., Sancar, A., and Kaufmann, W. K. (2007) *Mol. Cell. Biol.* **27,** 3131–3142
26. Errico, A., Costanzo, V., and Hunt, T. (2007) *Proc. Natl. Acad. Sci. U. S. A.* **104,** 14929–14934
27. Chou, D. M., and Elledge, S. J. (2006) *Proc. Natl. Acad. Sci. U. S. A.* **103,** 18143–18147
28. Yoshizawa-Sugata, N., and Masai, H. (2007) *J. Biol. Chem.* **282,** 2729–2740
29. Ünsal-Kaçmaz, K., Mullen, T. E., Kaufmann, W. K., and Sancar, A. (2005) *Mol. Cell. Biol.* **25,** 3109
30. Goss, K. H., Risinger, M. A., Kordich, J. J., Sanz, M. M., Straughen, J. E., Slovek, L. E., Capobianco, A. J., German, J., Boivin, G. P., and Groden, J. (2002) *Science* **297,** 2051–2053
31. Rijkers, T., Van Den Ouweland, J., Morolli, B., Rolink, A. G., Baarends, W. M., Van Sloun, P. P., Lohman, P. H., and Pastink, A. (1998) *Mol. Cell. Biol.* **18,** 6423–6429
32. Yu, Y., and Alwine, J. C. (2002) *J. Virol.* **76,** 3731–3738
33. Liu, Y., and Maizels, N. (2000) *EMBO Rep.* **1,** 85–90
34. Sarbassov, D. D., Guertin, D. A., Ali, S. M., and Sabatini, D. M. (2005) *Science* **307,** 1098–1101
35. Dull, T., Zufferey, R., Kelly, M., Mandel, R., Nguyen, M., Trono, D., and Naldini, L. (1998) *J. Virol.* **72,** 8463
36. Xiao, J., Li, C., Zhu, N. L., Borok, Z., and Minoo, P. (2003) *Dev. Dyn.* **228,** 82–94
37. Brown, E. J., and Baltimore, D. (2003) *Genes Dev.* **17,** 615–628
38. Rogakou, E. P., Pilch, D. R., Orr, A. H., Ivanova, V. S., and Bonner, W. M. (1998) *J. Biol. Chem.* **273,** 5858–5868
39. Mirzoeva, O. K., and Petrini, J. H. J. (2003) *Mol. Cancer Res.* **1,** 207–218
40. Haber, J. E. (1999) *Trends Biochem. Sci.* **24,** 271–275
41. West, S. C. (2003) *Nat. Rev. Mol. Cell Biol.* **4,** 435–445
42. Mortensen, U. H., Bendixen, C., Sunjevaric, I., and Rothstein, R. (1996) *Proc. Natl. Acad. Sci. U. S. A.* **93,** 10729–10734
43. Ogawa, T., Yu, X., Shinohara, A., and Egelman, E. H. (1993) *Science* **259,** 1896–1899
44. Chaganti, R. S., Schonberg, S., and German, J. (1974) *Proc. Natl. Acad. Sci. U. S. A.* **71,** 4508–4512
45. Amor-Gueret, M. (2006) *Cancer Lett.* **236,** 1–12
46. Ellis, N. A., Groden, J., Ye, T. Z., Straughen, J., Lennon, D. J., Ciocci, S., Proytcheva, M., and German, J. (1995) *Cell* **83,** 655–666
47. Karow, J. K., Constantinou, A., Li, J. L., West, S. C., and Hickson, I. D. (2000) *Proc. Natl. Acad. Sci. U. S. A.* **97,** 6504–6508
48. Wu, L., and Hickson, I. D. (2003) *Nature* **426,** 870–874
49. Davies, S. L., North, P. S., Dart, A., Lakin, N. D., and Hickson, I. D. (2004) *Mol. Cell. Biol.* **24,** 1279–1291
50. Sengupta, S., Robles, A. I., Linke, S. P., Sinogeeva, N. I., Zhang, R., Pedeux, R., Ward, I. M., Celesta, A., Nussenzweig, A., Chen, J., Halazonetis, T. D., and Harris, C. C. (2004) *J. Cell Biol.* **166,** 801–813
51. McDaniel, L. D., Chester, N., Watson, M., Borowsky, A. D., Leder, P., and Schultz, R. A. (2003) *DNA Repair* **2,** 1387–1404
52. Chester, N., Kuo, F., Kozak, C., O'Hara, C. D., and Leder, P. (1998) *Genes Dev.* **12,** 3382–3393
53. Gudmundsdottir, K., and Ashworth, A. (2006) *Oncogene* **25,** 5864–5874
54. Nagaraju, G., and Scully, R. (2007) *DNA Repair* **6,** 1018–1031
55. Heller, R. C., and Marians, K. J. (2006) *Nat. Rev. Mol. Cell Biol.* **7,** 932–943
56. Pan, X., Ye, P., Yuan, D. S., Wang, X., Bader, J. S., and Boeke, J. D. (2006) *Cell* **124,** 1069–1081
57. Henry-Mowatt, J., Jackson, D., Masson, J. Y., Johnson, P. A., Clements, P. M., Benson, F. E., Thompson, L. H., Takeda, S., West, S. C., and Caldecott, K. W. (2003) *Mol. Cell* **11,** 1109–1117
58. Yamaguchi-Iwai, Y., Sonoda, E., Buerstedde, J. M., Bezzubova, O., Morrison, C., Takata, M., Shinohara, A., and Takeda, S. (1998) *Mol. Cell. Biol.* **18,** 6430–6435
59. Fujimori, A., Tachiiri, S., Sonoda, E., Thompson, L. H., Dhar, P. K., Hiraoka, M., Takeda, S., Zhang, Y., Reth, M., and Takata, M. (2001) *EMBO J.* **20,** 5513–5520
60. McIlwraith, M. J., and West, S. C. (2008) *Mol. Cell* **29,** 510–516
61. Thorpe, P. H., Marrero, V. A., Savitzky, M. H., Sunjevaric, I., Freeman, T. C., and Rothstein, R. (2006) *Mol. Cell. Biol.* **26,** 3752–3763
62. Kuhn, E. M., and Therman, E. (1986) *Cancer Genet. Cytogenet.* **22,** 1–18